PEGylation Extends Circulation Half-Life While Preserving *In Vitro* and *In Vivo* Activity of Tissue Inhibitor of Metalloproteinases-1 (TIMP-1)

Jyotica Batra[9], Jessica Robinson[9¤], Christine Mehner, Alexandra Hockla, Erin Miller, Derek C. Radisky, Evette S. Radisky*

Department of Cancer Biology, Mayo Clinic Cancer Center, Jacksonville, Florida, United States of America

Abstract

Excess proteolytic activity of matrix metalloproteinases (MMPs) contributes to the development of arthritis, cardiovascular diseases and cancer progression, implicating these enzymes as therapeutic targets. While many small molecule inhibitors of MMPs have been developed, clinical uses have been limited, in part by toxicity and off-target effects. Development of the endogenous tissue inhibitors of metalloproteinases (TIMPs) as recombinant biopharmaceuticals represents an alternative therapeutic approach; however, the short plasma half-life of recombinant TIMPs has restricted their potential in this arena. To overcome this limitation, we have modified recombinant human TIMP-1 (rhTIMP-1) by PEGylation on lysine residues. We analyzed a mixture of mono- and di-PEGylated rhTIMP-1 species modified by attachment of 20 kDa mPEG chains (PEG$_{20K}$-TIMP-1), as confirmed by SELDI-TOF mass spectrometry. This preparation retained complete inhibitory activity toward the MMP-3 catalytic domain and partial inhibitory activity toward full length MMP-9. Pharmacokinetic evaluation showed that PEGylation extended the plasma half-life of rhTIMP-1 in mice from 1.1 h to 28 h. In biological assays, PEG$_{20K}$-TIMP-1 inhibited both MMP-dependent cancer cell invasion and tumor cell associated gelatinase activity. Overall these results suggest that PEGylated TIMP-1 exhibits improved potential for development as an anti-cancer recombinant protein therapeutic, and additionally may offer potential for clinical applications in the treatment of other diseases.

Introduction

The **m**atrix **m**etallo**p**roteinases (MMPs) are a family of 23 zinc-dependent endopeptidases with important functions in tissue morphogenesis, wound healing, and other physiological processes that require remodeling of the extracellular matrix [1,2,3,4]. MMP activity is regulated *in vivo* by a family of four endogenous protein protease inhibitors, the **t**issue **i**nhibitors of **m**etallo**p**roteinases (TIMPs), that bind to MMPs in 1:1 stoichiometry and block the protease active site [5,6]. Disruption of the balance between MMPs and TIMPs is evidenced under many pathological conditions, and excess MMP activity has long been recognized for important contributions to the development and progression of many diseases including cardiovascular, vascular, and pulmonary diseases, arthritis, multiple sclerosis, and cancer [2,7,8,9,10].

Diverse roles in disease development and progression have led MMPs to be regarded as promising therapeutic targets, resulting in development of many small-molecule MMP inhibitors, but clinical trials of early-generation MMP inhibitors in cancer and arthritis proved disappointing [11,12,13,14]. Broad-spectrum MMP inhibitors produced serious dose-limiting musculoskeletal toxicity, failed to reach therapeutic plasma levels, and failed to extend progression-free survival in cancer trials [11,12,14]; these disappointing outcomes have been attributed both to the toxicity and off-target effects of the drugs and to inadequate specificity for target MMPs.

A less toxic alternative to synthetic MMP inhibitors might be offered by TIMPs. Studies using many preclinical cancer models have shown that overexpression of natural TIMPs in tumors often leads to reduced tumor growth and metastasis [15]. Systemic gene transfer of TIMPs in animal models of cancer has likewise produced antitumor effects, with minimal toxicity [15]. In a handful of studies investigating the suppressive effect of TIMP-1 on tumor cell proliferation and metastasis, mice have been treated with recombinant human TIMP-1 (rhTIMP-1) protein at doses of 2–50 mg/kg with no reported toxicity [16,17,18,19]. Recombinant human TIMPs -1 and -2 have also been investigated as inhibitors of airway inflammation in a murine model of asthma, via intranasal instillation, with promising results [20].

For many applications, one barrier that will likely need to be addressed for TIMPs to enter the clinic as recombinant therapeutics is the short half-life in circulation of these small

proteins. Persistence in the circulation is desirable because protein therapeutics generally cannot be administered orally and typically are administered by subcutaneous, intramuscular, or intravenous injection or infusion. Animal studies using recombinant TIMPs have thus far been limited in part by rapid clearance of the protein; the plasma clearance of murine TIMP-1 in rats was reported to occur within minutes [21], and the blood elimination half-life of human TIMP-1 in mice was reported to be ~4 hours [22].

Chemical modification has been used to improve the pharmacokinetic profiles of several protein therapeutics now in the clinic [23,24,25,26]; one successful strategy is PEGylation, the covalent conjugation of polyethylene glycol chains to a protein. In general, PEGylation reduces renal clearance, increases circulatory half-life by a factor of 5–100-fold, and improves biological activity; it may also confer resistance to proteolysis and reduce immunogenicity [23,24]. While some PEGylated molecules demonstrate decreased binding in vitro to their natural ligands or receptors, these effects tend to be offset in vivo, with striking improvements in functional pharmacodynamic properties [23,24]. Furthermore, losses in target affinity can sometimes be minimized by site-directed PEGylation [23]; for example, by chemical conjugation of activated PEG to an unpaired cysteine residue introduced through genetic engineering [27,28].

TIMP-1 is a potent biological inhibitor of MMPs including MMP-9 (gelatinase B), a metalloproteinase that has been implicated as a potential therapeutic target in a wide variety of inflammatory and vascular diseases and in cancer [29]. Here, we tested several approaches to the covalent PEGylation of rhTIMP-1, and evaluated PEGylated rhTIMP-1 for retention of MMP inhibitory activity in biochemical and biological assays, as well as the impact of PEGylation on circulation half-life in mice.

Materials and Methods

Ethics Statement

Animal studies were carried out in strict accordance with the recommendations in the Guide for the Care and Use of Laboratory Animals of the National Institutes of Health. Mice were maintained following approved Mayo Clinic Institutional Animal Care and Use Committee protocols A12409 and A23108. Surgery was performed under avertin anesthesia, acetaminophen was administered throughout the preoperative and postoperative period, and all efforts were made to minimize suffering. For the serial blood withdrawals in the pharmacokinetic study, care was taken not to exceed the guidelines recommended by NIH for non-terminal blood withdrawal from rodents.

Recombinant Proteins

Mature secreted full-length rhTIMP-1 was expressed using the pTT/TIMP-1 construct transfected into HEK 293E cells [30], and was purified by SP-Sepharose chromatography as we have described previously [31]. Four mutant pTT/TIMP-1 constructs were generated to introduce a free Cys residue (R180C, S181C, Q182C, and A184C) using the Stratagene QuikChange mutagenesis kit (Agilent Technologies, Wilmington, DE, USA) according to the manufacturer's protocols. TIMP-1-R180C was the most highly expressed mutant in small scale studies; this mutant was produced in large scale for PEGylation studies and purified either by (a) SP-Sepharose chromatography in 50 mM 2-(N-morpholino)ethanesulfonic acid (MES), pH 6.0, using a linear gradient of 0–0.5 M NaCl, or (b) Q-Sepharose chromatography in 20 mM ethanolamine, pH 9.0, using a linear gradient of 0–0.5 M NaCl. Eluted fractions containing the rhTIMP-1 or rhTIMP-1-R180C

were assessed by silver stained SDS-PAGE. Recombinant human MMP-3 catalytic domain (MMP-3cd) was expressed in *E. coli*, purified, refolded, and activated as described previously [31,32]. Full-length recombinant human MMP-9 was purchased from Calbiochem, San Diego, CA, USA.

Conjugation of PEG to rhTIMP-1-R180C via Cys Residues

The rhTIMP-1-R180C mutant protein (~11 µM) was incubated in test reactions with 1.5–50-fold molar excess of freshly dissolved monomethoxypolyethylene glycol (mPEG)- maleimide of molecular weight 30K (Laysan Bio Inc, Arab, AL) in 100 mM sodium phosphate at pH 6, pH 7, or pH 8 at room temperature for 15 min –24 h. Prior to some incubations, the rhTIMP-1-R180C protein was pre-treated with the following reducing agents for 10 min –1 hr at room temperature or 37°C with or without inclusion of 2.5 M urea: 1.25–5-fold molar excess of TCEP, 50–200 µM DTT, 0.1–10 mM 2-mercaptoethylamine (MEA), bead-immobilized TCEP (Pierce Biotechnology, Rockford, IL, USA), or bead-immobilized DTT (Cleland's Reductacryl reagent, Calbiochem). Reducing agents were removed using a mini protein desalting spin column (Pierce) prior to test PEGylations. The degree of PEG incorporation into protein was assessed by observing molecular weight shifts on 10% SDS-polyacrylamide gels; proteins were visualized by silver staining and PEG was visualized by barium iodide staining [33]. Briefly, gels were washed twice with water, incubated with 5% $BaCl_2$ for 10 min, and then developed with 0.1 N iodine solution. Retention of MMP inhibitory activity by rhTIMP-1-R180C following partial reduction and/or PEGylation was assessed in assays measuring inhibition of MMP-3cd.

Conjugation of PEG to rhTIMP-1 via Lys Residues

Activated mPEG-succinimidyl carboxymethyl ester (mPEG-SCM) of molecular weight 5K and 20K (Jenkem Technologies, Allen, TX, USA) were dissolved in dry DMSO to make stock solutions of 40 mM and 10 mM, respectively. Wild-type rhTIMP-1 protein (~13 µM) was incubated in test reactions with 2–100-fold molar excess of $mPEG_{5K}$-SCM or 1–5-fold molar excess of $mPEG_{20K}$-SCM in 100 mM sodium phosphate at pH 8 or pH 8.5, at room temperature for 30 min –1 h. The degree of PEG incorporation into protein and retention of MMP inhibitory activity were assessed as described above. For larger scale PEGylation reactions, rhTIMP-1, at a concentration of 1 mg/ml quantified by UV absorbance at 280 nm and confirmed by BCA protein assay kit (Pierce), was dialysed into 100 mM sodium phosphate, pH 8.0. The rhTIMP-1 protein was incubated with 5-fold molar excess of $mPEG_{20K}$-SCM or 100-fold molar excess $mPEG_{5K}$-SCM for 30 minutes at room temperature.

To purify PEG_{20K}-TIMP-1, the PEGylation reaction was diluted in buffer A (50 mM MES, pH 6.0) to reduce the DMSO concentration to 1.5% and then resolved by SP-Sepharose chromatography. Unreacted rhTIMP-1, PEG_{20K}-TIMP-1 and $mPEG_{20K}$-SCM hydrolysis products were separated using a linear gradient of buffer B (50 mM MES, pH 6.0+0.5 M NaCl). A similar approach was used to purify PEG_{5K}-TIMP-1 but with both buffers at pH 5.0. Purity and extent of PEGylation was assessed on 10% SDS-polyacrylamide gels silver stained for protein and stained with barium iodide for PEG [33], as described above. Concentrations for unmodified and PEGylated TIMP preparations were determined by UV absorbance at 280 nm using a Nanodrop spectrophotometer (Thermo Fisher Scientific, Wilmington, DE, USA) using the predicted molar extinction coefficient of 26,190 $M^{-1}cm^{-1}$ which was calculated using the ExPASy ProtParam tool [34]. Retention of MMP inhibitory

activity by PEG_{20K}-TIMP-1 and PEG_{5K}-TIMP-1 was assessed in assays measuring inhibition of MMP-3cd. PEG_{20K}-TIMP-1 was also evaluated for inhibitory activity *versus* full-length recombinant human MMP-9.

Mass Spectrometry

Distribution of PEGylated species in preparations of PEG_{20K}-TIMP-1 and PEG_{5K}-TIMP-1 was analyzed on a Bio-Rad ProteinChip SELDI time-of-flight system. Protein samples at 1 mg/ml were mixed in 1:4 protein-to-matrix volume with the matrix (saturated sinapinic acid in 50% acetonitrile and 0.1% trifluoroacetic acid), and spotted (1 µL) onto a SELDI ProteinChip Gold Array (A-H Format, Bio-Rad). The mass-charge ratios (m/z) of TIMP-PEG species were determined using external calibration standards, All-In-One Protein Standards II (Bio-Rad) consisting of recombinant hirudin (7 kDa), cytochrome c (12 kDa), myoglobin (17 kDa), carbonic anhydrase (29 kDa), enolase (47 kDa), albumin (66 kDa) and IgG proteins (147 kDa).

MMP Inhibition Assays

The activities of PEGylated TIMP-1 species were assessed in MMP inhibition assays monitoring cleavage of the MMP thiopeptolide substrate Ac-Pro-Leu-Gly-S-Leu-Leu-Gly-OEt (Enzo Life Sciences, Plymouth Meeting, PA, USA) as previously described [31]. Briefly, mixtures of MMP-3cd and varying molar ratios of PEGylated or unmodified rhTIMP-1 were preincubated at 37°C for 2h and then mixed with substrate (100 µM) in assay buffer (50 mM HEPES, pH 6.0, 10 mM $CaCl_2$, 0.05% Brij-35) containing 1 mM 5,5′-dithiobis(2-nitrobenzoic acid). Linear initial rates were measured continuously as the increase in absorbance at 412 nm on a Varian Cary 100 spectrophotometer (Varian Inc, Palo Alto, CA) or on an Agilent 8453 spectrophotometer (Agilent Technologies, Santa Clara, CA, USA). The final enzyme concentration in the assay was 5 nM. Assays for inhibition of MMP-9 were conducted similarly, except that the assay buffer was at pH 7.0 and the final enzyme concentration in the reaction was 1 nM. The molar equivalents of unmodified or PEGylated rhTIMP-1 required to fully inhibit MMP activities were obtained from slopes fitted using linear regression with Prism 4 (GraphPad Software, San Diego, CA, USA).

Cell Culture

Human MDA-MB-231-luc2 breast cancer cells (Caliper Life Sciences, Hopkinton, MA, USA) were grown in Eagle's MEM medium with 10% FBS at 37°C in 5% CO_2 to 80% confluency [35]. RMF/EG human mammary fibroblasts, derived from a reduction mammoplasty and immortalized with human telomere and GFP [36], were a gift from Charlotte Kuperwasser, Tufts University, Boston, MA, USA. RMF/EG fibroblasts were cultured in DMEM medium containing 10% bovine calf serum and 1% penicillin/streptomycin to 80% confluency.

Matrigel Transwell Invasion Assays

MDA-MB-231-luc2 cells were split and replated at a density of 2×10^6 cells per 100 mm dish on the day before the assay. Cells (2.5×10^4 per well in 500 µL Eagle's MEM containing 0.1% BSA) were plated into a BD BioCoat Matrigel Invasion Chamber 24 well plate with 8.0 µm PET membrane (BD Falcon, Franklin Lakes, NJ, USA). The lower chambers contained 750 µL/well of NIH/3T3 cell conditioned serum free medium (DMEM supplemented with 50 µg/mL ascorbic acid) as chemo-attractant. Some wells included either rhTIMP-1 or PEG_{20K}-TIMP-1 at 50 nM or 500 nM; each condition was represented by 3 replicate wells.

Assays were incubated 18 h at 37°C in 5% CO_2. Non-invading cells were removed from the insert by scrubbing with a cotton swab, and then cells on the lower surface of the filter were fixed with methanol, stained with crystal violet, and counted using Image-Pro 6.3 software (Media Cybernetics) as previously described [37].

In Situ Zymography

In situ zymography techniques were modified from previously published protocols [38,39,40]. For *in situ* zymography of cultured RMF/EG mammary fibroblasts, 2×10^4 cells were grown overnight in 500 µL DMEM on 8-well chamber slides (Thermo Scientific, Waltman, MA, USA) at 37°C with 5% CO_2 under humidified conditions. Incubation solutions containing 50 µg/mL DQ-gelatin (Thermo Scientific) and 1 µg/mL Hoechst 33258 (Invitrogen, Grand Island, NY, USA) were prepared in 1×PBS, with or without 500 nM PEG_{20K}-TIMP-1. After removing the media from the cells, 60 µL of incubation solution was added drop-wise to each chamber well to cover all cells. Slides were kept protected from light at room temperature for 1 h, and then examined by fluorescence microscopy and photographed. DQ-gelatin cleavage by gelatinases was visualized using the GFP-channel; GFP expression by the fibroblasts produced a barely detectable background signal, against which the brighter de-quenched fluorescein signal from cleaved DQ-gelatin was clearly detected.

For *in situ* zymography of frozen tumor sections, tissue was cryosectioned at −20°C, mounted onto glass slides, and then thawed slowly on ice. An incubation solution containing 100 µg/mL DQ-gelatin and 1 µg/mL Hoechst 33258 in 1×PBS was pre-mixed and equilibrated to 42°C just before mixing with an equal volume of 2% low melting agarose. Incubation solution/agarose (40 µL) was carefully spread over the thawed tissue. Slides were covered from light and placed at 4°C for 5 minutes for the agarose to solidify, followed by 3 hours incubation at room temperature. DQ-gelatin cleavage by gelatinases was assessed via microscopy as described above.

Pharmacokinetic Study

Mice (6 per group) were injected intraperitoneally with 2 mg/kg rhTIMP-1 or PEG_{20K}-TIMP-1. This dose was selected because it is a dose that for rhTIMP-1 has been shown to have an antitumorigenic effect in a xenograft model of colon cancer [19], and in our preliminary studies we confirmed our ability to detect the resultant blood concentration of rhTIMP-1 by ELISA. To minimize the number of mice and quantity of recombinant protein required, blood collections were performed serially using previously described techniques [41,42,43]. Mice were placed in a mouse tail illuminator (Braintree Scientific Inc, Braintree, MA, USA) and the tail cleaned with alcohol. After locating a suitable vein, the area was covered with petroleum jelly and a small incision made with a 22½ gauge needle. A 20 µL sample was collected using a heparinized capillary tube and dispensed into a pre-weighed microvette tube precoated with EDTA (Sarstedt, Newton, NC, USA). Within each injection group, mice were divided into two subgroups of 3 (A and B subgroups) which were bled at alternating time points to avoid exceeding recommended volume limits for non-terminal blood withdrawal. For the rhTIMP-1 group mice were bled at 0 min (A and B), 30 min (A), 45 min (B), 1 h (A), 1.5 h (B), 2 h (A), 2.5 h (B), 3 h (A), 4 h (A), 6 h (B), and 8 h (B). For the PEG_{20K}-TIMP-1 group mice were bled at 0 min (A and B), 1 h (A), 2 h (B), 3 h (A), 4 h (B), 6 h (A), 8 h (B), 12 h (A), 24 h (A), 48 h (B), and 72 h (B). At the final

time point each mouse was terminally bled by cardiac puncture and ~1 mL of blood was collected.

Blood samples were diluted with 10 volumes 0.1 M trisodium citrate to inhibit coagulation and centrifuged to pellet red blood cells, and then the plasma supernatant was collected and frozen at −30°C until analyzed. Concentrations of TIMP-1 and PEG_{20K}-TIMP-1 were quantified using a Human TIMP-1 ELISA kit (Bender MedSystems, San Diego, CA) according to the manufacturer's instructions, using the manufacturer provided rhTIMP-1 as well as our lab-produced rhTIMP-1 and PEG_{20K}-TIMP-1 to generate standard curves. This kit was found to be highly sensitive for both rhTIMP-1 and PEG_{20K}-TIMP-1, and to have minimal cross-reactivity with mouse TIMP-1. The dynamic range for detection of rhTIMP-1 and PEG_{20K}-TIMP-1 was 39–2500 pg/mL; these concentrations were achieved in plasma samples after an additional 50–500-fold dilution in the assay (after the initial 10-fold dilution). Standard curves were fit to data for 8 rhTIMP-1 concentrations run in duplicate, using a four-parameter sigmoidal (logistic) model ($R^2 > 0.99$), and concentrations in plasma were determined from duplicate assays by nonlinear interpolation from the standard curve, using Prism version 4.0 (GraphPad Software, La Jolla, CA, USA). The data were displayed as a semilogarithmic plot and fitted to the equation for two phase exponential decay using Prism version 4.0 to obtain the best fit values for distribution and elimination; values were excluded for rhTIMP-1 for the 30 min and 45 min time points, where the measured values exceeded the quantifiable range of the assay.

Mammary Orthotopic Xenograft Study

A mixture of 1×10^5 MDA-MB-231-luc2 human breast cancer cells and 1×10^5 human mammary fibroblasts in 25 µL serum-free Eagle's MEM medium plus 25 µL growth factor-reduced phenol red-free Matrigel was injected into the inguinal mammary gland of 6–10-week-old female Nod/LtSz-prkds(scid) (NOD/SCID) mice (Jackson Laboratory, Bar Harbor, ME, USA). Tumors were allowed to grow over the course of 11 weeks, monitored weekly by bioluminescence imaging using an IVIS Spectrum 3-dimensional imaging system (Caliper Life Sciences).

PEG_{20K}-TIMP-1 was dialyzed into PBS, filter sterilized, and protein concentration was determined by UV absorbance at 280 nm using a Nanodrop spectrophotometer (Thermo Fisher Scientific, Wilmington, DE, USA). At 11 weeks post-implantation, two tumor-bearing mice were injected intraperitoneally with 2 mg/kg PEG_{20K}-TIMP-1 and two tumor-bearing mice were injected with 0.9% saline only. This dose was selected because it is a dose that for rhTIMP-1 has been shown to have an antitumorigenic effect in a xenograft model of colon cancer [19]. Twenty four hours later, all four mice were euthanized by CO_2 inhalation, and tumors were resected and flash frozen in liquid N_2 and stored at −80°C until analysis. MMP activity was assessed in fresh-frozen tumors by *in situ* zymography as described above.

Results

In considering how best to approach PEGylation of rhTIMP-1, we analyzed the structure of the protein and its mode of interaction with an MMP catalytic domain (**Fig. 1**) [31,44]. TIMP-1 is a globular protein of 184 amino acids and is glycosylated on two Asn residues. It possesses 12 Cys residues, paired as 6 disulfide bonds, and 8 Lys residues. The most common approach to protein PEGylation involves coupling of activated PEGs to primary amines found on Lys side chains and at the protein N-terminus [45]. In the case of TIMP-1, the N-terminal amine is absolutely essential for activity, because it inserts into the

active site cleft of the protease and directly coordinates to the catalytic zinc (**Fig. 1**); this interaction is the basis for inhibition of MMPs by TIMPs. Any modification of the natural TIMP N-terminus, even extension by a single Ala residue, will destroy antiprotease activity [46], and mutations that disrupt the N-terminal disulfide bond between Cys-1 and Cys-70 are similarly destructive [47,48]. To avoid the risk of N-terminal PEGylation, and to direct PEG attachment to a site distant from the TIMP-MMP interface, our first approach was to introduce a single unpaired Cys residue near the flexible C-terminus of TIMP-1, opposite the MMP-binding face, for reaction with a thiol-reactive PEG.

Conjugation of PEG to rhTIMP-1 via an Introduced Cys Residue

To facilitate site-specific PEGylation of rhTIMP-1, we made four mutants each introducing a Cys residue near the C-terminus (**Fig. 1**) and tested expression levels in the HEK 293E mammalian expression system, finding highest expression for the R180C mutant (**Fig. S1A**). The rhTIMP-1-R180C was produced in larger scale, purified, and analyzed under nonreducing conditions, which showed that while some disulfide dimers were present, the major species was monomeric (**Fig. S1B**), with the introduced Cys presumed to be available for modification. An mPEG-maleimide reagent of molecular weight 30K was selected with the rationale
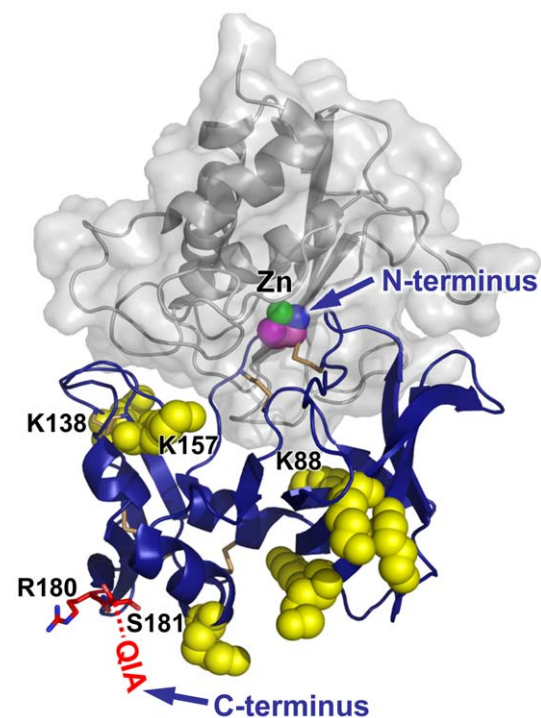
Figure 1. TIMP-1 sites of inhibitory interaction and PEGylation. TIMP-1 (blue) is shown binding to the MMP-3 catalytic domain (gray); the N-terminal Cys-1 backbone (magenta and blue spheres) coordinates directly to the MMP catalytic Zn (green). The C-terminal residues Arg-180, Ser-181, Gln-182, and Ala-184 (red sticks; residues 182–184 unstructured in the crystal structure) were initially mutated to Cys and targeted for site-specific PEGylation. In a subsequent approach, the 8 natural Lys residues (yellow spheres) were targeted for PEGylation. Lys-138, Lys-157 and Lys-88 all lie within 10 Å of the MMP-3 cd, while other Lys residues are distant from the binding interface. Structure coordinates are from PDB ID 1UEA [44]; figure was created using PyMOL.

doi:10.1371/journal.pone.0050028.g001
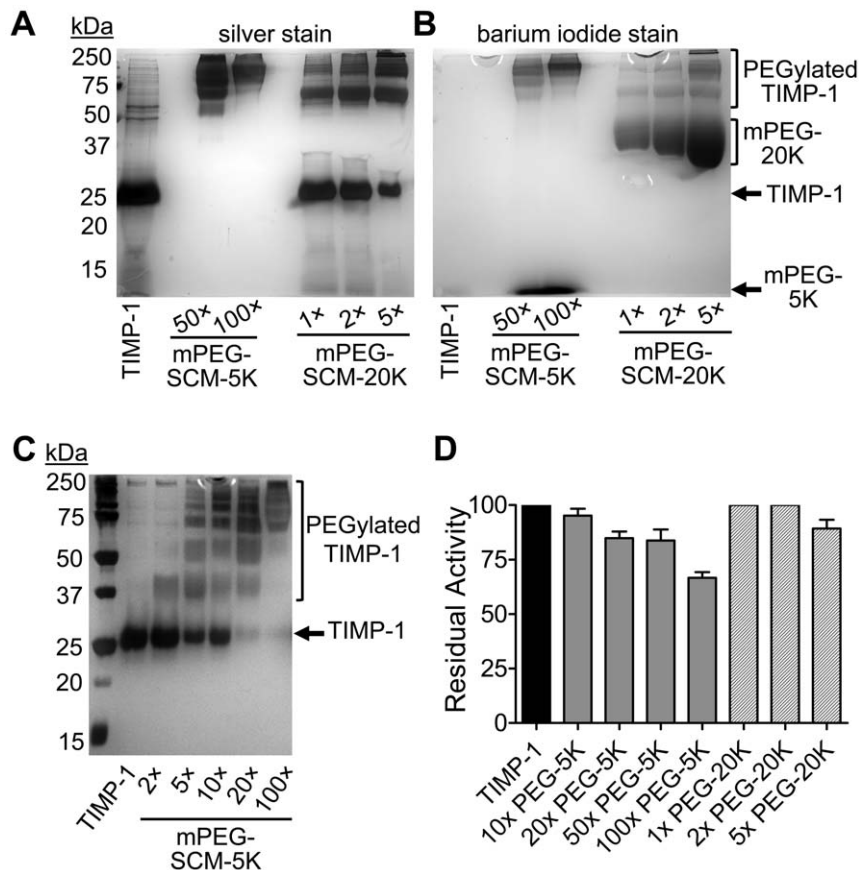
Figure 2. PEGylation on rhTIMP-1 Lys residues with mPEG-SCM reagents. (A) Silver stained gel shows unmodified rhTIMP-1 and PEGylation reactions carried out in the presence of 50–100× molar excess of mPEG-SCM-5K or 1–5× molar excess of mPEG-SCM-20K, as indicated beneath gel. (B) The same gel stained with barium iodide shows the electrophoretic migration of mPEG-5K and mPEG-20K hydrolysis products and PEGylated rhTIMP-1 species. (C) Silver stained gel shows a concentration-dependent increase in molecular weight upon PEGylation with mPEG-5K-SCM in increasing molar excess. (D) Graph shows retention of MMP-3cd inhibitory activity relative to rhTIMP-1 by PEGylated rhTIMP-1 species from the reactions shown in panels A-C. The molar excess over rhTIMP-1 and molecular weight of the activated PEG in each reaction is indicated below the gel.
doi:10.1371/journal.pone.0050028.g002

that attachment of a single very large PEG substituent would likely be sufficient to prevent rapid renal elimination.

Reaction conditions were tested using a variety of PEG:protein molar ratios, pH ranges, temperatures, and reaction times. Surprisingly, we failed to detect rhTIMP-1-R180C PEGylation under any conditions. We verified 100% reactivity of the purchased mPEG-maleimide by titration against cysteine using Ellman's reagent (5,5′-dithiobis-(2-nitrobenzoic acid) to quantify residual free cysteine. We next hypothesized that failure of rhTIMP-1-R180C to react could be attributable either to (a) inaccessibility of Cys-180 caused by the fold of the protein, or (b) covalent blockage of Cys-180 by disulfide formation with small sulfhydryl compounds. To distinguish between these possibilities, we carried out test reactions in the presence of urea to partially denature the protein, alleviating steric hindrance, or TCEP, a disulfide reductant unreactive with mPEG-maleimide. Inclusion of TCEP resulted in complete PEGylation while urea denaturation had little effect, suggesting that the difficulties in PEGylating rhTIMP-1-R180C were caused solely by Cys oxidation.

In an attempt to identify regioselective conditions for partial reduction that would allow deprotection of Cys-180 without disrupting the native disulfide bonds essential for TIMP-1 activity [47,48], we tested a wide variety of reducing agents and conditions, assessing both the effectiveness of PEGylation and the retention of MMP inhibitory activity following reduction. As summarized in **Table S1**, regardless of the reducing agent employed, conditions resulting in efficient PEGylation of rhTIMP-1-R180C also severely compromised MMP inhibitory activity. We concluded that PEGylation on Cys-180 of the mutant rhTIMP-1 was incompatible with retention of activity.

Conjugation of PEG to rhTIMP-1 via Native Lys Residues

As an alternative approach for PEGylation of rhTIMP-1, we attempted to identify conditions under which Lys residues on the surface of the protein could be modified with minimal disruption of activity. Because the free N-terminal amine is vital for the inhibitory function of TIMP-1, conditions were optimized to favor modification on Lys residues and to avoid modification of the N-terminus. There are 8 Lys residues in TIMP-1 which could potentially serve as sites of modification (**Fig. 1**). The majority are located distant from the MMP interface where modification would not be expected to interfere with activity; however, Lys-88, Lys-138, and Lys-157, with respective distances of 8Å, 5Å, and 6Å from a bound MMP catalytic domain, could conceivably hinder MMP binding upon PEGylation. We therefore tested the impact on rhTIMP-1 activity of modification by two molecular weights of activated amine reactive mPEG (mPEG-SCM-5K and mPEG-

SCM-20K) under conditions allowing varying degrees of PEGylation.

We observed a concentration-dependent increase in PEGylation (both fraction of protein PEGylated and molecular weight distribution the of PEGylated species) with increasing molar excess of reagents mPEG-SCM-5K or mPEG-SCM-20K (**Fig. 2A–C**). Reactions were assessed by SDS-PAGE, evaluating by silver staining the change in apparent molecular weight of rhTIMP-1 protein upon modification (**Fig. 2A,C**) and confirming by barium iodide staining the incorporation of PEG into the higher molecular weight protein species (**Fig. 2B**). In reactions with mPEG-SCM-5K, essentially all rhTIMP-1 became PEGylated in the presence of 20×or greater molar excess of reagent (**Fig. 2A,C**). Activity tests showed retention of >80% MMP inhibitory activity in PEGylation with 20×or 50×excess reagent and 67% activity with 100×excess reagent (**Fig. 2D**). For mPEG-SCM-20K, the greatest molar excess of reagent achieved was 5×, yielding a mixture of mono- and di-PEGylated species with 10–20% residual unreacted rhTIMP-1 (**Fig. 2A**); this mixture retained 90% of the original activity (**Fig. 2D**).

Production and Characterization of PEG$_{5K}$-TIMP-1 and PEG$_{20K}$-TIMP-1

Larger scale PEGylation reactions were carried out using 100×molar excess of mPEG-SCM-5K or 5×molar excess of mPEG-SCM-20K, and PEGylated proteins were purified by ion exchange chromatography. Preparations were assessed by SDS-PAGE, where the purified PEG$_{20K}$-TIMP-1 revealed a very slight degree of contamination with unmodified rhTIMP-1 (**Fig. 3A**). In activity assays testing the inhibitory activity of the PEGylated TIMP preparations against the MMP-3 catalytic domain (MMP-3cd) when incubated in a 0.8:1.0 molar ratio, PEG$_{5K}$-TIMP-1 inhibited MMP activity by 80%, identical to unmodified rhTIMP-1 and consistent with 1:1 stoichiometry of inhibition, indicating full retention of inhibitory activity (**Fig. 3B**). Surprisingly, the PEG$_{20K}$-TIMP-1 preparation inhibited MMP activity to an even greater extent, revealing activity greater than that calculated for 100% activity (**Fig. 3B**). Since it does not seem plausible that the 1:1 stoichiometry of inhibition will have changed upon PEGylation, we conclude that the discrepancy is likely due to an underestimate of protein concentration in this PEGylated preparation as determined by absorbance measurements at 280 nm. PEGylation does not alter the calculated molar extinction coefficient, but it is possible that the presence of PEG chains at specific sites on rhTIMP-1 alter the chromophore microenvironment of one or more specific aromatic residues, resulting in small changes to the measured extinction coefficient of the natively folded protein.

We also compared PEG$_{20K}$-TIMP-1 to rhTIMP-1 for inhibition of full-length recombinant human MMP-9. We found that whereas 1.0 molar equivalent of rhTIMP-1 effectively quenches the activity of MMP-9, 1.9 molar equivalents of PEG$_{20K}$-TIMP-1 would be required to achieve the same effect (**Fig. 3C**). This suggests that the PEG$_{20K}$-TIMP-1 preparation represents a heterogenous mixture of PEGylated species, in which nearly half of the molecules are PEGylated at a site deleterious for MMP-9 binding. In addition to binding the catalytic domain of MMP-9, TIMP-1 binds to the C-terminal hemopexin domain of MMP-9 and proMMP-9. Although the precise structural nature of this contact is not known, it appears to involve the C-terminal subdomain of TIMP-1 [49,50]. Our data suggest that, independently of its effect on MMP catalytic domain binding, TIMP-1 PEGylation might interfere with this secondary interaction and thus alter the specific ability of TIMP-1 to inhibit intact MMP-9.
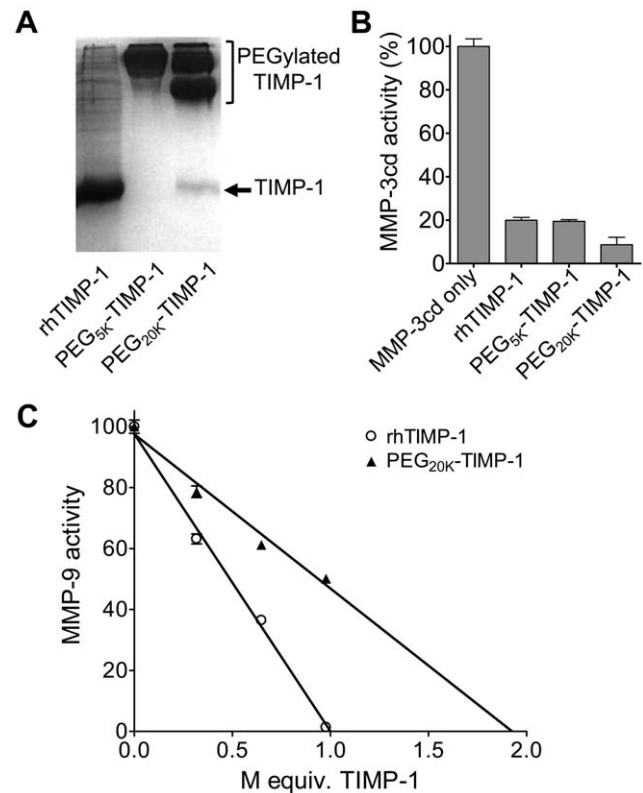

Figure 3. MMP inhibitory activity of PEGylated rhTIMP-1. (A) Silver stained gel shows purified rhTIMP-1, PEG$_{5K}$ -TIMP-1, and PEG$_{20K}$ -TIMP-1. Reactions were carried out using 100× molar excess of mPEG-SCM-5K or 5× molar excess of mPEG-SCM-20K, and PEGylated protein species were purified by ion exchange chromatography. (B) Graph shows inhibition of MMP-3cd by 0.8 molar equivalent of rhTIMP-1, PEG$_{5K}$ -TIMP-1 or PEG$_{20K}$ -TIMP-1. Protein concentrations were calculated from absorbance measurements using predicted molar extinction coefficients. (C) Graph shows titration of a fixed concentration of full-length recombinant human MMP-9 by increasing molar equivalents of rhTIMP-1 and PEG$_{20K}$-TIMP-1.
doi:10.1371/journal.pone.0050028.g003

Next, we analyzed the distribution of PEGylated species in the PEG$_{5K}$-TIMP-1 and PEG$_{20K}$-TIMP-1 preparations by surface enhanced laser desorption/ionization (SELDI) time-of-flight mass spectrometry. The mass peak for rhTIMP-1 was centered at 24,775 Da (**Fig. 4A**), consistent with the calculated protein mass of 20,709 Da and the two confirmed sites of N-linked glycosylation [51]. For PEG$_{5K}$-TIMP-1, peaks were centered at 46529 Da, 51657 Da, 567951 Da and 62101 Da, confirming the conjugation of 4–7 molecules, respectively, of mPEG-SCM-5K; the most abundant species was that featuring attachment of 5 PEG chains (**Fig. 4B**). For PEG$_{20K}$-TIMP-1, peaks were centered at 45139 Da and 65476 Da, confirming the conjugation of 1–2 molecules of mPEG-SCM-20K, with a predominance of mono-PEGylation; a peak for the residual unmodified rhTIMP-1 was present as well (**Fig. 4C**).

PEGylation Extends rhTIMP-1 Plasma Half-life in Mice

We carried out a pharmacokinetic study in mice to compare the circulation half-life of unmodified and PEGylated rhTIMP-1, which were quantified in plasma using an ELISA assay specific for human TIMP-1. In preliminary studies we found that PEG$_{20K}$-TIMP-1 was detected with similar sensitivity to rhTIMP-1, whereas the more extensively modified PEG$_{5K}$-TIMP-1 was
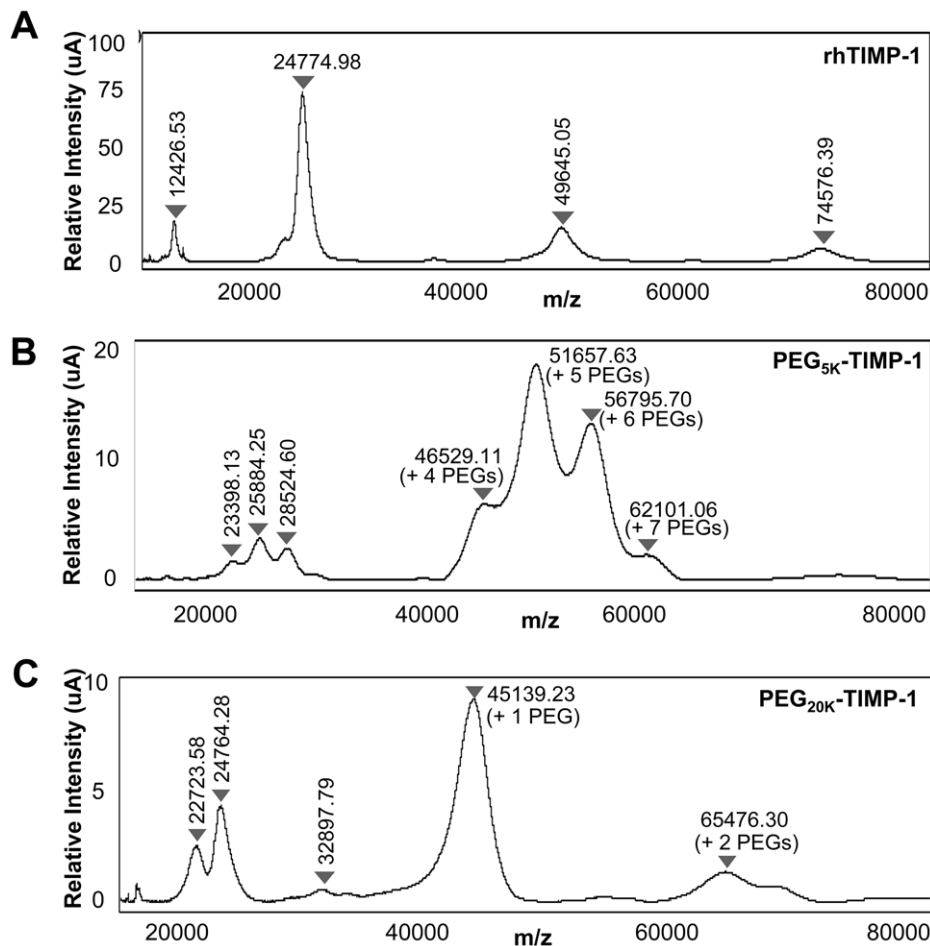
Figure 4. SELDI MS for rhTIMP-1 and PEGylated preparations. (A) SELDI time-of-flight mass spectrum of unmodified rhTIMP-1 shows a molecular mass of 24,775 Da. (B) Mass spectrum of PEG$_{5K}$-TIMP-1 shows a molecular mass range of 46,529 Da –62,101 Da, indicating conjugation of 4–7 mPEG-5K chains; the most abundant species possesses 5 mPEG-5K chains. The smaller peaks in the range of 23,398–28,524 are consistent with doubly charged ions of the PEGylated species bearing 4–6 mPEG chains. (C) Mass spectrum of PEG$_{20K}$-TIMP-1 shows a molecular mass range of 45,139 Da –65,476 Da, indicating attachment of 1–2 mPEG-20K chains, with the mono-PEGylated species predominant. Doubly charged ions for the mono- and di-PEGylated species are also present, as is a peak for unmodified rhTIMP-1.
doi:10.1371/journal.pone.0050028.g004

detected with about 5-fold lower sensitivity; we therefore chose to focus on PEG$_{20K}$-TIMP-1 for the *in vivo* studies. Using an experimental design involving serial blood sampling of 6 mice per group, we compared the persistence in circulation of rhTIMP-1 *versus* PEG$_{20K}$-TIMP-1 after a single 2 mg/kg intraperitoneal injection (**Fig. 5**). For each series, data points were fitted by a two phase exponential decay model, yielding for rhTIMP-1 a distribution half-life of 0.22 h and an elimination half-life of 1.1 h; for PEG$_{20K}$-TIMP-1 the distribution half-life was 3.4 h and the elimination half-life was 28 h. These data indicate a 25-fold increase in terminal elimination half-life for the PEGylated TIMP-1. No toxicity or adverse effects were noted in the treated mice.

PEG$_{20K}$-TIMP-1 Inhibits MMP-dependent Cancer Cell Invasion and Tumor Cell-associated Gelatinase Activity

The ability of PEG$_{20K}$-TIMP-1 to inhibit MMP-dependent cancer cell invasion was evaluated in Matrigel transwell assays using MDA-MB-231 cells, a highly invasive cell line derived from a metastatic breast adenocarcinoma. The invasive behavior of these cells has been found to be highly dependent on MMPs [52]. Invasion was significantly decreased in a concentration dependent

fashion when assays were carried out in the presence of 50 or 500 nM unmodified or PEGylated rhTIMP-1 (**Fig. 6**). Surprisingly, PEG$_{20K}$-TIMP-1 was more effective than rhTIMP-1 for suppression of invasion (**Fig. 6**), despite the reported importance of MMP-9 for invasion in this model [53,54,55] and our data showing that MMP-9 inhibition is diminished by PEGylation. These results suggest the possibility that PEGylation may render TIMP-1 more stable against degradation in the cell culture environment.

To directly visualize the inhibition of MMP activity in the cellular environment, we carried out *in situ* zymography experiments with human mammary fibroblasts, which secrete high levels of MMP-2 and moderate levels of MMP-9. Using this technique, pericellular gelatinase activity is imaged through cleavage of the quenched fluorogenic substrate DQ-gelatin. While control cultures showed clear evidence of gelatinase activity as indicated by green fluorescence surrounding the cells (**Fig. 7A**, left), greatly reduced gelatinase activity was evidenced in cultures treated with 500 nM PEG$_{20K}$-TIMP-1 (**Fig. 7B**, right).

The ability of the PEG$_{20K}$-TIMP-1 to inhibit tumor-associated MMP activity was also evaluated in mice bearing orthotopic xenograft mammary tumors. Because complex interactions
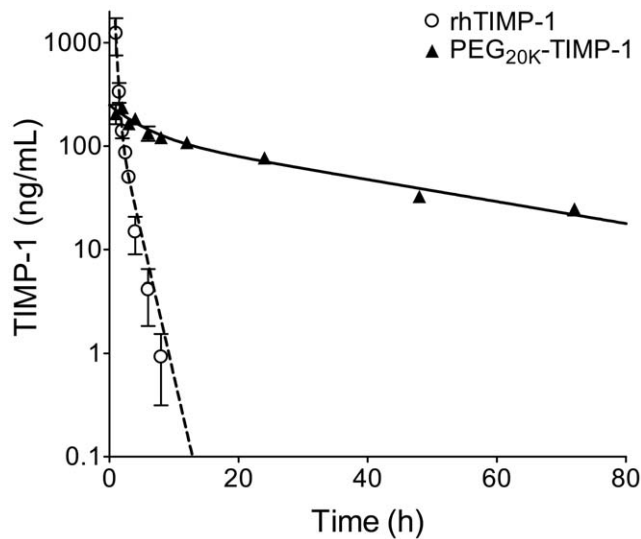
Figure 5. PEG$_{20K}$-TIMP-1 *versus* rhTIMP-1 plasma half-life. Semilogarithmic plot of rhTIMP-1 (open circles) or PEG$_{20K}$-TIMP-1 (filled triangles) in plasma *versus* time show that half-life is markedly extended for the PEGylated protein. Mice (6 per group) were injected intraperitoneally with 2 mg/kg rhTIMP-1 or PEG$_{20K}$-TIMP-1 and then blood samples were collected serially at the indicated time points; each data point represents the average and standard error for measurements from 3 mice. The dotted and solid curves show best fits to the equation for two phase exponential decay for rhTIMP-1 and PEG$_{20K}$-TIMP-1, respectively.
doi:10.1371/journal.pone.0050028.g005

between tumor cells and stromal fibroblasts stimulate MMP production at the invasive front in both types of cells [39,56,57,58,59,60], we chose to employ a physiologically relevant model in which human MDA-MB-231 tumor cells and human mammary fibroblasts were co-implanted into the mammary fat pad of immunocompromised mice. Tumors were allowed to grow for 11 weeks, mice bearing similarly sized tumors were then injected with a single dose of either 2 mg/kg PEG$_{20K}$-TIMP-1 or saline only, and MMP activity was assessed by *in situ* zymography in the fresh-frozen tumors harvested 24 h later. Because of the very short elimination half-life observed for rhTIMP-1 in the pharmacokinetic study (**Fig. 5**), we did not include rhTIMP-1 as a control in the tumor targeting study, anticipating that it would show little effect after 24 h *in vivo*. *In situ* zymography of tumors from control mice injected with saline showed gelatinase activity that was most concentrated near the periphery of the tumors (**Fig. 7B**, left), while tumors from PEG$_{20K}$-TIMP-1-injected mice showed noticeably diminished evidence of gelatinase activity associated with the tumor (**Fig. 7B**, right). This experiment suggests that injected PEG$_{20K}$-TIMP-1 is localized to tumors, where it persists at least 24 hours after injection and effectively suppresses gelatinase activity *in vivo* in tumor tissue.

Discussion

MMPs remain therapeutic targets of interest for cancer and for many other diseases. Recombinant TIMPs represent an as yet underexplored source of biologics that could be developed for clinical uses targeting MMPs. Therapeutics derived from human proteins offer a number of advantages over small-molecule drugs, including greater specificity and low toxicity [61], however they often come with a unique set of challenges with regard to formulation, delivery, *in vivo* stability, short circulation half-life,
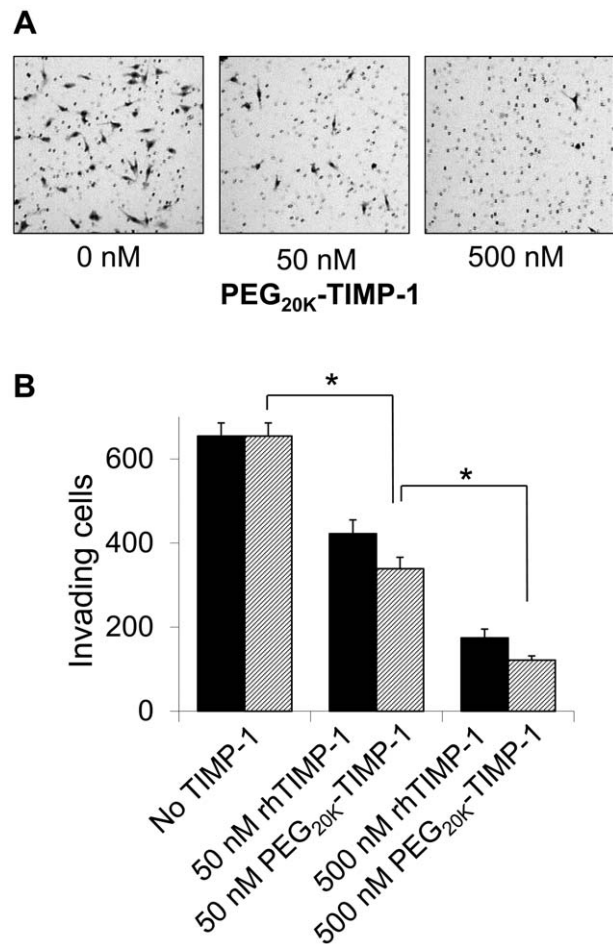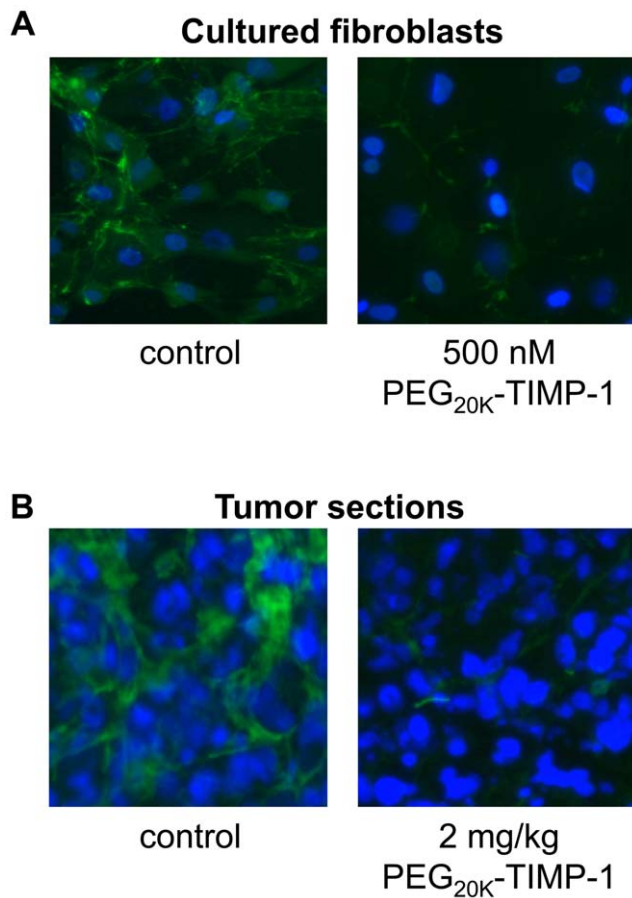

Figure 6. PEG$_{20K}$-TIMP-1 activity in cancer cell invasion assay. (A) Pictures of representative fields from filters with fixed and stained cells are shown for control and PEG$_{20K}$-TIMP-1-treated wells. (B) Graph shows a concentration dependent decrease in the number of invasive MDA-MB-231 cells in the presence of 50 or 500 nM of unmodified or PEGylated rhTIMP-1 in Matrigel transwell assays. Plotted values represent average and standard error from triplicate filters; cells were counted from entire filters using image processing software. *, $p < 0.01$.
doi:10.1371/journal.pone.0050028.g006

and rapid clearance [23]. Here, we pursued PEGylation as an approach to overcome the short plasma half-life of rhTIMP-1 and developed methodology for limited PEGylation on Lys side chains of rhTIMP-1 with preservation of MMP inhibitory activity. We found that the resultant PEG$_{20K}$-TIMP-1 preparation inhibited MMP activity *in vitro* and *in vivo*, and was capable of inhibiting cancer cell invasion with improved potency.

Previous reports of unmodified rhTIMP-1 pharmacokinetics in rodents have varied considerably; an early study found an elimination half-life of 4 h in mice [22], while another group recently reported a half-life of 42 h in an ischemia-reperfusion model in rats [62]. Both of these values are considerably longer than the 1.1 h elimination half-life that we measured for rhTIMP-1 (**Fig. 5**). Major differences include (a) that both prior studies employed ^{125}I-labelled rhTIMP-1 to follow distribution and clearance while we used an ELISA with high specificity for human TIMP-1, and (b) that the prior studies administered much lower doses (μg/kg rather than mg/kg). A caveat in the interpretation of radiolabelling studies is that the assay does not specifically monitor intact or active rhTIMP-1 molecules, but

A   Cultured fibroblasts

control

500 nM
PEG$_{20K}$-TIMP-1

B   Tumor sections

control

2 mg/kg
PEG$_{20K}$-TIMP-1

Figure 7. MMP inhibitory activity of PEG$_{20K}$-TIMP-1 in fibroblast cultures and orthotopic tumors. (A) *In situ* zymography of mammary fibroblast cultures developed with (right panel) or without (left panel) 500 nM PEG$_{20K}$-TIMP-1 show decreased gelatinase activity in the treated cells, as indicated by a reduction in green fluorescent signal produced by cleavage of quenched fluorescent substrate DQ-gelatin. (B) *In situ* zymography of tumor sections from mammary tumor-bearing mice injected 24 hours prior to sacrifice with saline (left) or 2 mg/kg PEG$_{20K}$-TIMP-1 (right) show reduced gelatinase activity in the tumor from the mouse receiving PEG$_{20K}$-TIMP-1.
doi:10.1371/journal.pone.0050028.g007

would detect partially degraded polypeptide fragments of rhTIMP-1 as well. Indeed, electrophoretic analysis of ^{125}I-labelled rhTIMP-1 in the rat ischemia-reperfusion model showed that the signal for intact protein peaked at 1.5 h and was much diminished by 3 h [62]. By contrast, we would anticipate that the ELISA used in our experiment would provide a more specific readout for intact biologically active TIMP-1, and therefore a more meaningful measurement from the perspective of therapeutic utility. Our pharmacokinetic study showed gradual elimination of PEG$_{20K}$-TIMP-1 over the course of several days (**Fig. 5**); this is consistent with our *in situ* zymography results (**Fig. 7B**), which suggest that substantial inhibitory activity is retained *in vivo* even after 24 h.

TIMP-1 and its modified derivatives may be particularly well suited for therapeutic targeting of MMP-9, a potential drug target in many pathological processes. MMP-9 has been implicated in atherosclerotic plaque rupture, tissue damage after acute myocardial infarction, and breakdown of the blood-brain barrier and development of brain edema after cerebral ischemia and in other CNS conditions [29]. It also plays significant roles promoting cancer invasion, metastasis, and angiogenesis, as well as inflam-

matory diseases including osteoarthritis, rheumatoid arthritis, multiple sclerosis, chronic obstructive pulmonary disease (COPD) and other conditions of pulmonary inflammation and fibrosis [29,63,64]. Among TIMPs, native TIMP-1 has the strongest preexisting affinity for MMP-9 [50,65,66], and possesses the unique ability to bind to proMMP-9 through an interaction between the C-terminal domain of TIMP-1 and the C-terminal hemopexin (PEX) domain of the proenzyme [49,50]. This high-affinity interaction substantially accelerates the kinetics of MMP-9/TIMP-1 association [50], likely contributing to selectivity of TIMP-1 toward MMP-9 *in vivo*. The N-terminal domain of TIMP-1 in the proMMP-9/TIMP-1 complex remains available and competent for inhibiting other active MMP molecules including MMP-3 [67,68], a physiological activator of MMP-9 [69,70]; the interaction with TIMP-1 therefore protects proMMP-9 from enzymatic activation *in vitro* [67,71] and *in vivo* [72]. While native TIMP-1 therefore offers special advantages where targeting of MMP-9 is desired, we found that the PEG$_{20K}$-TIMP-1 preparation inhibited MMP-9 somewhat less effectively than it inhibited MMP-3cd. This was possibly due to steric incompatibility between one or more sites of TIMP-1 lysine PEGylation and the MMP-9 PEX domain. For retention of optimal activity toward MMP-9, it may be advantageous for future studies to further pursue approaches for more regioselective PEGylation of rhTIMP-1. Although we did not find success with PEGylation of an introduced Cys residue, the most common approach toward site-specific PEGylation, another possible approach might pursue PEGylation on the two glycosyl groups of TIMP-1, both of which lie within the N-terminal domain and well removed from the inhibitory site. Yet another possibility could involve mutational studies to identify which of the TIMP-1 Lys residues interferes with MMP-9 association upon PEGylation, and then specifically removing that site of modification by mutagenesis.

TIMP-1 offers a potential biopharmaceutical MMP inhibitor but is rapidly eliminated; our results indicate that PEGylation is one feasible approach to improve its pharmacokinetic profile while preserving activity. Several recent publications have suggested other biopharmaceutical approaches to MMP inhibition. Nanoparticles loaded with mouse TIMP-1 were shown to provide neuroprotection in an organotypic hippocampal slice culture model [73]. A fusion protein formed from human TIMP-2 and human serum albumin was found to provide an improved pharmacokinetic profile and biodistribution in a tumor model and to provide an antiangiogenic effect [74]. Furthermore, TIMPs are not the only biomolecules to be investigated as scaffolds for development of MMP inhibitors. An inhibitory human antibody targeting MMP-14, developed using phage display technology, has shown *in vivo* activity in mouse xenograft tumor models [75]. Mouse monoclonal antibodies, raised against a synthetic antigen that mimics the MMP catalytic site, were shown to inhibit gelatinases via a TIMP-like binding mechanism, and to show therapeutic promise in a mouse model of inflammatory bowel disease [76]. The methods tested and developed in the present work will contribute to the developing biotechnological arsenal for creating next-generation MMP inhibitors.

Supporting Information

Figure S1   Expression and characterization of rhTIMP-1 Cys Mutant R180C. (a) Silver stained gel shows varying levels of recombinant TIMP in conditioned media from expression cultures for different rhTIMP-1 Cys mutants, as indicated above the gel. (b) Non-reducing SDS-PAGE and Western blot of purified rhTIMP-

1-R180C show that the predominant species present is monomeric.
(TIF)

Table S1 Effect of partially reducing conditions on MMP inhibitory activity and PEGylation.
(DOCX)

Acknowledgments

We thank Terrone Rosenberry and Brenda Moore for assistance with SELDI-MS. We thank Charlotte Kuperwasser for the gift of RMF/EG

Author Contributions

Conceived and designed the experiments: JB JR CM AH DCR ESR. Performed the experiments: JB JR CM AH EM. Analyzed the data: JB JR CM AH EM DCR ESR. Wrote the paper: JB JR CM DCR ESR.

References

1. Stamenkovic I (2003) Extracellular matrix remodelling: the role of matrix metalloproteinases. J Pathol 200: 448–464.
2. Murphy G, Nagase H (2008) Progress in matrix metalloproteinase research. Mol Aspects Med 29: 290–308.
3. Gill SE, Parks WC (2008) Metalloproteinases and their inhibitors: regulators of wound healing. International Journal of Biochemistry and Cell Biology 40: 1334–1347.
4. Radisky ES, Radisky DC (2010) Matrix metalloproteinase-induced epithelial-mesenchymal transition in breast cancer. J Mammary Gland Biol Neoplasia 15: 201–212.
5. Brew K, Dinakarpandian D, Nagase H (2000) Tissue inhibitors of metalloproteinases: evolution, structure and function. Biochim Biophys Acta 1477: 267–283.
6. Murphy G (2011) Tissue inhibitors of metalloproteinases. Genome Biology 12: 233.
7. Hu J, Van den Steen PE, Sang QX, Opdenakker G (2007) Matrix metalloproteinase inhibitors as therapy for inflammatory and vascular diseases. Nat Rev Drug Discov 6: 480–498.
8. Kessenbrock K, Plaks V, Werb Z (2010) Matrix metalloproteinases: regulators of the tumor microenvironment. Cell 141: 52–67.
9. Vandenbroucke RE, Dejonckheere E, Libert C (2011) A therapeutic role for matrix metalloproteinase inhibitors in lung diseases? European Respiratory Journal 38: 1200–1214.
10. Newby AC (2012) Matrix metalloproteinase inhibition therapy for vascular diseases. Vascular Pharmacology 56: 232–244.
11. Coussens LM, Fingleton B, Matrisian LM (2002) Matrix metalloproteinase inhibitors and cancer: trials and tribulations. Science 295: 2387–2392.
12. Turk B (2006) Targeting proteases: successes, failures and future prospects. Nat Rev Drug Discov 5: 785–799.
13. Burrage PS, Brinckerhoff CE (2007) Molecular targets in osteoarthritis: metalloproteinases and their inhibitors. Curr Drug Targets 8: 293–303.
14. Fingleton B (2008) MMPs as therapeutic targets-Still a viable option? Semin Cell Dev Biol 19: 61–68.
15. Brand K (2002) Cancer gene therapy with tissue inhibitors of metalloproteinases (TIMPs). Curr Gene Ther 2: 255–271.
16. Schultz RM, Silberman S, Persky B, Bajkowski AS, Carmichael DF (1988) Inhibition by human recombinant tissue inhibitor of metalloproteinases of human amnion invasion and lung colonization by murine B16-F10 melanoma cells. Cancer Res 48: 5539–5545.
17. Alvarez OA, Carmichael DF, DeClerck YA (1990) Inhibition of collagenolytic activity and metastasis of tumor cells by a recombinant human tissue inhibitor of metalloproteinases. J Natl Cancer Inst 82: 589–595.
18. Yamauchi K, Ogata Y, Nagase H, Shirouzu K (2001) Inhibition of liver metastasis from orthotopically implanted colon cancer in nude mice by transfection of the TIMP-1 gene into KM12SM cells. Surg Today 31: 791–798.
19. Ohtani Y, Aoe M, Hara F, Tao H, Koshimune R, et al. (2006) Suppression effects of human recombinant tissue inhibitor of metalloproteinases-1(TIMP-1) on tumor proliferation using in vivo treatment model of well-differentiated colon cancer cell line, HT29. Acta Med Okayama 60: 257–266.
20. Kumagai K, Ohno I, Okada S, Ohkawara Y, Suzuki K, et al. (1999) Inhibition of matrix metalloproteinases prevents allergen-induced airway inflammation in a murine model of asthma. J Immunol 162: 4212–4219.
21. Kurschat P, Graeve L, Erren A, Gatsios P, Rose-John S, et al. (1995) Expression of a biologically active murine tissue inhibitor of metalloproteinases-1 (TIMP-1) in baculovirus-infected insect cells. Purification and tissue distribution in the rat. Eur J Biochem 234: 485–491.
22. Black RA, Durie FH, Otten-Evans C, Miller R, Slack JL, et al. (1996) Relaxed specificity of matrix metalloproteinases (MMPS) and TIMP insensitivity of tumor necrosis factor-alpha (TNF-alpha) production suggest the major TNF-alpha converting enzyme is not an MMP. Biochem Biophys Res Commun 225: 400–405.
23. Harris JM, Chess RB (2003) Effect of pegylation on pharmaceuticals. Nat Rev Drug Discov 2: 214–221.
24. Harris JM, Martin NE, Modi M (2001) Pegylation: a novel process for modifying pharmacokinetics. Clin Pharmacokinet 40: 539–551.
25. Szymkowski DE (2005) Creating the next generation of protein therapeutics through rational drug design. Curr Opin Drug Discov Devel 8: 590–600.
26. Veronese FM, Harris JM (2008) Peptide and protein PEGylation III: advances in chemistry and clinical applications. Adv Drug Deliv Rev 60: 1–2.
27. Goodson RJ, Katre NV (1990) Site-directed pegylation of recombinant interleukin-2 at its glycosylation site. Biotechnology (N Y) 8: 343–346.
28. Pepinsky RB, Shapiro RI, Wang S, Chakraborty A, Gill A, et al. (2002) Long-acting forms of Sonic hedgehog with improved pharmacokinetic and pharmacodynamic properties are efficacious in a nerve injury model. J Pharm Sci 91: 371–387.
29. Van den Steen PE, Dubois B, Nelissen I, Rudd PM, Dwek RA, et al. (2002) Biochemistry and molecular biology of gelatinase B or matrix metalloproteinase-9 (MMP-9). Critical Reviews in Biochemistry and Molecular Biology 37: 375–536.
30. Crombez L, Marques B, Lenormand JL, Mouz N, Polack B, et al. (2005) High level production of secreted proteins: example of the human tissue inhibitor of metalloproteinases 1. Biochem Biophys Res Commun 337: 908–915.
31. Batra J, Robinson J, Soares AS, Fields AP, Radisky DC, et al. (2012) Matrix metalloproteinase-10 (MMP-10) interaction with tissue inhibitors of metalloproteinases TIMP-1 and TIMP-2: binding studies and crystal structure. J Biol Chem 287: 15935–15946.
32. Suzuki K, Kan CC, Hung W, Gehring MR, Brew K, et al. (1998) Expression of human pro-matrix metalloproteinase 3 that lacks the N-terminal 34 residues in Escherichia coli: autoactivation and interaction with tissue inhibitor of metalloproteinase 1 (TIMP-1). Biol Chem 379: 185–191.
33. Kurfürst MM (1992) Detection and molecular weight determination of polyethylene glycol-modified hirudin by staining after sodium dodecyl sulfate-polyacrylamide gel electrophoresis. Analytical Biochemistry 200: 244–248.
34. Gasteiger E, Hoogland C, Gattiker A, Duvaud S, Wilkins MR, et al. (2005) Protein Identification and Analysis Tools on the ExPASy Server. In: Walker JM, editor. The Proteomics Protocols Handbook. Totowa, N.J.: Humana Press. 571–607.
35. Jenkins DE, Hornig YS, Oei Y, Dusich J, Purchio T (2005) Bioluminescent human breast cancer cell lines that permit rapid and sensitive in vivo detection of mammary tumors and multiple metastases in immune deficient mice. Breast Cancer Res 7: R444–454.
36. Kuperwasser C, Chavarria T, Wu M, Magrane G, Gray JW, et al. (2004) Reconstruction of functionally normal and malignant human breast tissues in mice. Proc Natl Acad Sci U S A 101: 4966–4971.
37. Salameh MA, Soares AS, Hockla A, Radisky DC, Radisky ES (2011) The P(2)′ residue is a key determinant of mesotrypsin specificity: engineering a high-affinity inhibitor with anticancer activity. Biochem J 440: 95–105.
38. Mook OR, Van Overbeek C, Ackema EG, Van Maldegem F, Frederiks WM (2003) In situ localization of gelatinolytic activity in the extracellular matrix of metastases of colon cancer in rat liver using quenched fluorogenic DQ-gelatin. Journal of Histochemistry and Cytochemistry 51: 821–829.
39. Stuelten CH, DaCosta Byfield S, Arany PR, Karpova TS, Stetler-Stevenson WG, et al. (2005) Breast cancer cells induce stromal fibroblasts to express MMP-9 via secretion of TNF-alpha and TGF-beta. J Cell Sci 118: 2143–2153.
40. Snock-van Beurden PA, Von den Hoff JW (2005) Zymographic techniques for the analysis of matrix metalloproteinases and their inhibitors. Biotechniques 38: 73–83.
41. Abatan OI, Welch KB, Nemzek JA (2008) Evaluation of saphenous venipuncture and modified tail-clip blood collection in mice. J Am Assoc Lab Anim Sci 47: 8–15.
42. Bateman KP, Castonguay G, Xu L, Rowland S, Nicoll-Griffith DA, et al. (2001) Reduction of animal usage by serial bleeding of mice for pharmacokinetic studies: application of robotic sample preparation and fast liquid chromatography-mass spectrometry. J Chromatogr B Biomed Sci Appl 754: 245–251.
43. Durschlag M, Wurbel H, Stauffacher M, Von Holst D (1996) Repeated blood collection in the laboratory mouse by tail incision–modification of an old technique. Physiol Behav 60: 1565–1568.
44. Gomis-Ruth FX, Maskos K, Betz M, Bergner A, Huber R, et al. (1997) Mechanism of inhibition of the human matrix metalloproteinase stromelysin-1 by TIMP-1. Nature 389: 77–81.

45. Roberts MJ, Bentley MD, Harris JM (2002) Chemistry for peptide and protein PEGylation. Adv Drug Deliv Rev 54: 459–476.

46. Wingfield PT, Sax JK, Stahl SJ, Kaufman J, Palmer I, et al. (1999) Biophysical and functional characterization of full-length, recombinant human tissue inhibitor of metalloproteinases-2 (TIMP-2) produced in Escherichia coli. Comparison of wild type and amino-terminal alanine appended variant with implications for the mechanism of TIMP functions. J Biol Chem 274: 21362–21368.

47. Huang W, Meng Q, Suzuki K, Nagase H, Brew K (1997) Mutational study of the amino-terminal domain of human tissue inhibitor of metalloproteinases 1 (TIMP-1) locates an inhibitory region for matrix metalloproteinases. J Biol Chem 272: 22086–22091.

48. Caterina NC, Windsor LJ, Yermovsky AE, Bodden MK, Taylor KB, et al. (1997) Replacement of conserved cysteines in human tissue inhibitor of metalloproteinases-1. J Biol Chem 272: 32141–32149.

49. Murphy G, Houbrechts A, Cockett MI, Williamson RA, O'Shea M, et al. (1991) The N-terminal domain of tissue inhibitor of metalloproteinase retains metalloproteinase inhibitory activity. Biochemistry 30: 8097–8102.

50. O'Connell JP, Willenbrock F, Docherty AJ, Eaton D, Murphy G (1994) Analysis of the role of the COOH-terminal domain in the activation, proteolytic activity, and tissue inhibitor of metalloproteinase interactions of gelatinase B. J Biol Chem 269: 14967–14973.

51. Ramachandran P, Boontheung P, Xie Y, Sondej M, Wong DT, et al. (2006) Identification of N-linked glycoproteins in human saliva by glycoprotein capture and mass spectrometry. Journal of Proteome Research 5: 1493–1503.

52. Radisky ES, Radisky DC (2007) Stromal induction of breast cancer: inflammation and invasion. Rev Endocr Metab Disord 8: 279–287.

53. Kunigal S, Lakka SS, Gondi CS, Estes N, Rao JS (2007) RNAi-mediated downregulation of urokinase plasminogen activator receptor and matrix metalloprotease-9 in human breast cancer cells results in decreased tumor invasion, angiogenesis and growth. Int J Cancer 121: 2307–2316.

54. Safina A, Ren MQ, Vandette E, Bakin AV (2008) TAK1 is required for TGF-beta 1-mediated regulation of matrix metalloproteinase-9 and metastasis. Oncogene 27: 1198–1207.

55. Safina A, Vandette E, Bakin AV (2007) ALK5 promotes tumor angiogenesis by upregulating matrix metalloproteinase-9 in tumor cells. Oncogene 26: 2407–2422.

56. Himelstein BP, Canete-Soler R, Bernhard EJ, Muschel RJ (1994) Induction of fibroblast 92 kDa gelatinase/type IV collagenase expression by direct contact with metastatic tumor cells. J Cell Sci 107 (Pt 2): 477–486.

57. Ito A, Nakajima S, Sasaguri Y, Nagase H, Mori Y (1995) Co-culture of human breast adenocarcinoma MCF-7 cells and human dermal fibroblasts enhances the production of matrix metalloproteinases 1, 2 and 3 in fibroblasts. British Journal of Cancer 71: 1039–1045.

58. Himelstein BP, Muschel RJ (1996) Induction of matrix metalloproteinase 9 expression in breast carcinoma cells by a soluble factor from fibroblasts. Clin Exp Metastasis 14: 197–208.

59. Saad S, Bendall LJ, James A, Gottlieb DJ, Bradstock KF (2000) Induction of matrix metalloproteinases MMP-1 and MMP-2 by co-culture of breast cancer cells and bone marrow fibroblasts. Breast Cancer Res Treat 63: 105–115.

60. Singer CF, Kronsteiner N, Marton E, Kubista M, Cullen KJ, et al. (2002) MMP-2 and MMP-9 expression in breast cancer-derived human fibroblasts is differentially regulated by stromal-epithelial interactions. Breast Cancer Res Treat 72: 69–77.

61. Leader B, Baca QJ, Golan DE (2008) Protein therapeutics: a summary and pharmacological classification. Nat Rev Drug Discov 7: 21–39.

62. Sa Y, Hao J, Samineni D, Clark J, Pyne-Geithman G, et al. (2011) Brain distribution and elimination of recombinant human TIMP-1 after cerebral ischemia and reperfusion in rats. Neurological Research 33: 433–438.

63. Egeblad M, Werb Z (2002) New functions for the matrix metalloproteinases in cancer progression. Nat Rev Cancer 2: 161–174.

64. Muroski ME, Roycik MD, Newcomer RG, Van den Steen PE, Opdenakker G, et al. (2008) Matrix metalloproteinase-9/gelatinase B is a putative therapeutic target of chronic obstructive pulmonary disease and multiple sclerosis. Curr Pharm Biotechnol 9: 34–46.

65. Olson MW, Gervasi DC, Mobashery S, Fridman R (1997) Kinetic analysis of the binding of human matrix metalloproteinase-2 and -9 to tissue inhibitor of metalloproteinase (TIMP)-1 and TIMP-2. J Biol Chem 272: 29975–29983.

66. Vempati P, Karagiannis ED, Popel AS (2007) A biochemical model of matrix metalloproteinase 9 activation and inhibition. J Biol Chem 282: 37585–37596.

67. Ogata Y, Itoh Y, Nagase H (1995) Steps involved in activation of the pro-matrix metalloproteinase 9 (progelatinase B)-tissue inhibitor of metalloproteinases-1 complex by 4-aminophenylmercuric acetate and proteinases. J Biol Chem 270: 18506–18511.

68. Kolkenbrock H, Orgel D, Hecker-Kia A, Zimmermann J, Ulbrich N (1995) Generation and activity of the ternary gelatinase B/TIMP-1/LMW-stromelysin-1 complex. Biol Chem Hoppe Seyler 376: 495–500.

69. Ogata Y, Enghild JJ, Nagase H (1992) Matrix metalloproteinase 3 (stromelysin) activates the precursor for the human matrix metalloproteinase 9. J Biol Chem 267: 3581–3584.

70. Ramos-DeSimone N, Hahn-Dantona E, Sipley J, Nagase H, French DL, et al. (1999) Activation of matrix metalloproteinase-9 (MMP-9) via a converging plasmin/stromelysin-1 cascade enhances tumor cell invasion. J Biol Chem 274: 13066–13076.

71. Goldberg GI, Strongin A, Collier IE, Genrich LT, Marmer BL (1992) Interaction of 92-kDa type IV collagenase with the tissue inhibitor of metalloproteinases prevents dimerization, complex formation with interstitial collagenase, and activation of the proenzyme with stromelysin. J Biol Chem 267: 4583–4591.

72. Ardi VC, Van den Steen PE, Opdenakker G, Schweighofer B, Deryugina EI, et al. (2009) Neutrophil MMP-9 proenzyme, unencumbered by TIMP-1, undergoes efficient activation in vivo and catalytically induces angiogenesis via a basic fibroblast growth factor (FGF-2)/FGFR-2 pathway. J Biol Chem 284: 25854–25866.

73. Chaturvedi M, Figiel I, Sreedhar B, Kaczmarek L (2012) Neuroprotection from Tissue Inhibitor of Metalloproteinase-1 and its nanoparticles. Neurochemistry International.

74. Lee MS, Kim YH, Kim YJ, Kwon SH, Bang JK, et al. (2011) Pharmacokinetics and biodistribution of human serum albumin-TIMP-2 fusion protein using near-infrared optical imaging. Journal of Pharmacy & Pharmaceutical Sciences 14: 368–377.

75. Devy L, Huang L, Naa L, Yanamandra N, Pieters H, et al. (2009) Selective inhibition of matrix metalloproteinase-14 blocks tumor growth, invasion, and angiogenesis. Cancer Res 69: 1517–1526.

76. Sela-Passwell N, Kikkeri R, Dym O, Rozenberg H, Margalit R, et al. (2012) Antibodies targeting the catalytic zinc complex of activated matrix metalloproteinases show therapeutic potential. Nature Medicine 18: 143–147.